Published in final edited form as:
J Magn Reson Imaging. 2011 September ; 34(3): 585–594. doi:10.1002/jmri.22713.

Optimized High-Resolution Contrast-Enhanced Hepatobiliary Imaging at 3T: A Cross-over Comparison of Gadobenate Dimeglumine and Gadoxetic Acid

Alex Frydrychowicz, MD[1,*], **Scott K. Nagle, MD, PhD**[1], **Sharon L. D'Souza, MD**[1], **Karl K. Vigen, PhD**[2], and **Scott B. Reeder, MD, PhD**[1,2,3,4]

[1] Department of Radiology, University of Wisconsin - Madison, WI

[2] Department of Medical Physics, University of Wisconsin - Madison, WI

[3] Department of Biomedical Engineering, University of Wisconsin - Madison, WI

[4] Department of Medicine, University of Wisconsin - Madison, WI

Abstract

Purpose—To evaluate the SNR and CNR performance of 0.05 mmol/kg gadoxetic acid and 0.1 mmol/kg gadobenate dimeglumine for dynamic and hepatobiliary phase imaging. In addition, flip angles (FA) that maximize relative contrast-to-noise performance for hepatobiliary phase imaging were determined.

Materials and Methods—A cross-over study in ten volunteers was performed using each agent. Imaging was performed at 3T with a 32-channel phased-array coil using breath-held 3D spoiled gradient echo sequences for SNR and CNR analysis, and for FA optimization of hepatobiliary phase imaging.

Results—Gadobenate dimeglumine (0.1 mmol/kg) had superior SNR performance during the dynamic phase, statistically significant for portal vein and hepatic vein in the portal venous and venous phase (for all, $p<0.05$) despite twice the approved dose of gadoxetic acid (0.05 mmol/kg), while gadoxetic acid had superior SNR performance during the hepatobiliary phase. Optimal FA's for hepatobiliary phase imaging using gadoxetic acid and gadobenate dimeglumine were 25–30° and 25–30° for relative contrast liver vs. muscle (surrogate for non-hepatocellular tissues), and 45° and 20° (relative contrast liver vs. biliary structures), respectively.

Conclusion—Gadobenate dimeglumine may be preferable for applications that require dynamic phase imaging only, while gadoxetic acid may be preferable when the hepatobiliary phase is clinically important. Hepatobiliary phase imaging with both agents benefits from flip angle optimization.

Keywords

Hepatobiliary imaging; gadoxetic acid; gadobenate dimeglumine; MR cholangiography

[*]Corresponding Author: Alex Frydrychowicz, MD, University of Wisconsin - Madison, Department of Radiology, 600 Highland Ave, CSC E1/322, Madison, WI 53727, Phone: 608-261-1865, Fax: 608-263-0876, frydrychowic@wisc.edu.

Disclosures: S.K.N., S.D'S., and K.K.V. have no disclosures. A.F. received an educational stipend from Bracco Diagnostics. S.B.R. previously served on the Medical Advisory Board for Bayer. The University of Wisconsin – Madison receives research support from Bracco and GE Healthcare.

INTRODUCTION

In recent years there has been increasing interest in the use of gadolinium based contrast agents with hepatobiliary uptake and excretion for improved characterization of liver lesions, detection of metastases (1–5) and for functional biliary imaging (6). Hepatobiliary contrast agents differ from conventional extracellular gadolinium-based contrast agents (GBCA) due to their uptake into functioning hepatocytes and subsequent excretion into bile. Two GBCA's with hepatobiliary uptake and excretion are currently approved in the U.S.A. and Europe: 1) gadoxetic acid (Eovist, Primovist; Gd-EOB-DTPA, Bayer Pharmaceuticals, Wayne, NJ, U.S.A.) and 2) gadobenate dimeglumine (MultiHance, Gd-BOPTA, Bracco Diagnostics, Princeton, U.S.A.). Both agents can be used for dynamic phase imaging (i.e.: have properties similar to conventional extracellular GBCA's), but are also taken up into functioning hepatocytes and excreted into bile. Approximately 50% of gadoxetic acid is taken up in the liver, while approximately 5% of gadobenate dimeglumine is taken up into the liver. Further, liver enhancement increases until it reaches a plateau beginning at 15–25 min using gadoxetic acid, and at 60–90 min using gadobenate dimeglumine (7–9).

The specific enhancement pattern and time course by which gadobenate dimeglumine and gadoxetic acid are taken up by hepatocytes and are secreted into the bile has been the subject of past studies (10). Several reports have investigated the performance of these agents separately (3,8,11), but there is a relative paucity of literature comparing them directly (7,12). Brismar et al. compared the hepatic vessel enhancement of 0.025 mmol/kg gadoxetic acid with 0.1 mmol/kg gadobenate dimeglumine and concluded that 0.025 mmol/kg gadoxetic acid did not offer equivalent vessel enhancement (12). Further, a recent comparison of both agents at 0.1 mmol/kg of gadobenate dimeglumine and 0.025 mmol/kg of gadoxetic acid by Lee et al. showed inferior vessel enhancement using gadoxetic acid (6), although this study was limited by the lack of a cross-over design. Similarly, Motosugi and coworkers compared 0.025 mol/kg and 0.05 mmol/kg gadoxetic acid in cirrhotic patients showed improved performance using 0.05 mmol/kg in patients with more advanced liver disease (higher Child-Pugh class) (13). Anecdotally, a similar behavior has been observed at our institution, and as a result, a weight-based dose of 0.05 mmol/kg is used in all patients to ensure adequate dynamic phase enhancement.

There are even less data available comparing gadoxetic acid and gadobenate dimeglumine at 3T. The *in-vitro* relaxivities of both agents show a similar small decrease with increasing field strength: the r_1 of gadobenate dimeglumine and gadoxetic acid are 6.9 L $mmol^{-1}$ s^{-1} and 6.2 L $mmol^{-1}$ s^{-1} at 1.5T, respectively, and 6.3 L $mmol^{-1}$ s^{-1} and 5.5 L $mmol^{-1}$ s^{-1} at 3T, respectively (14). Given these differences in relaxivity and large differences in pharmacokinetics, including weak binding of gadobenate dimeglumine to albumin, it may be difficult to extrapolate results at 1.5T to 3T, warranting additional comparisons at 3T.

Finally, sequence parameter optimization for hepatobiliary phase imaging using hepatobiliary gadolinium agents has drawn little attention, but has tremendous potential to improve image quality and better exploit the behavior of these agents. Although sequence optimization using GBCA's at higher field strengths has generally been shown to be beneficial for several areas of the body (15–19), no comparable study exists for hepatobiliary imaging. In clinical routine liver imaging at 1.5T, flip angles on the order of 12–15° are typically used for dynamic phase imaging. For hepatobiliary phase imaging, data from Nagle et al. suggested increasing the flip angle to 30–40° for hepatobiliary phase imaging with 0.05 mmol/kg gadoxetic acid at 1.5T (20). These initial results were confirmed by feasibility results in liver lesions at 1.5T by Bashir et al. (21). To the best of our knowledge, no flip angle optimization using either gadobenate dimeglumine or gadoxetic acid has been performed for hepatobiliary phase imaging at 3T.

Therefore, the purpose of this work was twofold: a) to compare the SNR and CNR performance of these agents during dynamic and hepatobiliary phase imaging at 3T, and b) to determine the optimum flip angles to maximize relative CNR performance of gadoxetic acid and gadobenate dimeglumine at 3T.

MATERIALS AND METHODS

Human Subjects and Injection Protocol

This HIPAA-compliant study had received institutional review board (IRB) approval prior to recruitment of volunteers. Ten healthy subjects (5: 5 male: female) aged 24.5 ± 3.7 years (21–33 years) weighing 67.6 ± 14.0 kg (52.2–92.9 kg) were recruited from an IRB-approved database of potential MRI scan volunteers at our institution. Informed written consent was obtained from each volunteer. Volunteers were asked to fast five hours before each scheduled examination per institutional routine for clinical MRCP and liver imaging.

Between October and December 2009, each volunteer was scanned on two separate days, once with gadobenate dimeglumine (0.1 mmol/kg) and once with gadoxetic acid (0.05 mmol/kg), in a random order for each volunteer. Injections were performed using a power injector (Spectris Solaris, MedRad Inc., Warendale, PA, USA) at 2 ml/s via a 20G antecubital intravenous catheter. The time interval between scans in each volunteer was 21.8 ± 12.3 days (6–47 days) to avoid the possibility of residual contrast within the biliary tract. Six volunteers received gadoxetic acid during their first scan, while four volunteers received gadobenate dimeglumine first.

MR Imaging

Imaging was performed on a 3T MR scanner (Discovery MR 750, GE Healthcare, Waukesha, WI, USA) using the 20 most superior elements of a 32-channel phased-array receive-only coil (NeoCoil, Pewaukee, WI, USA) centered on the upper abdomen of each subject in supine position. Two pulse sequence protocols were used 1) to assess SNR and CNR performance during the time course of enhancement, and 2) for flip angle optimization during the hepatobiliary phase. Acquisition parameters are summarized in Table 1, and sequences were acquired as follows (see also Figure 1):

Sequence 1 was acquired during the dynamic phase and the extended time course in order to measure SNR and CNR. Comparison of the SNR and CNR performance between the two contrast agents requires that absolute values of SNR and CNR be acquired. Therefore, it was necessary to avoid the use of parallel imaging, which would corrupt our ability to measure absolute SNR/CNR performance (22–23). Bolus timing for the arterial phase was performed using SmartPrep, a fluoroscopically triggered method for automatic bolus detection in the abdominal aorta (24). SmartPrep is the vendor-specific adaptation of this principle with low (<1 sec) delay from bolus detection to automated scan start. This was followed by imaging 50 seconds after the arterial phase for portal venous phase imaging, and at 2 min after injection for a venous phase. Imaging with sequence 1 was also repeated every 5 minutes starting at 10 minutes after the injection.

Sequence 2 was used for flip angle optimization. Parallel imaging using Autocalibrating Reconstruction for Cartesian imaging (ARC) (25) was used in sequence 2 in order to achieve high-resolution images and complete liver coverage within a single breath hold. High spatial resolution was necessary to ensure visualization of biliary structures without partial volume effects. Sequential acquisitions varying the flip angle by 5° increments from 15–45° were performed in all volunteers. A10° flip angle acquisition was added for six of the volunteers after preliminary data analysis indicated that an acquisition with 10° would

improve the dynamic range of the flip angle optimization. The timing of the studies for flip angle optimization was adapted to previously reported values of optimal contrast enhancement in the biliary: at 25–35 min after injection for gadoxetic acid (7–8) and 75–85 min for gadobenate dimeglumine (7,9).

Data Analysis – ROI Placement

Data analysis was performed offline using an Advantage Windows Workstation (GE Healthcare, Waukesha, WI, USA) by drawing regions of interest (ROI) in specific tissues of interest, copying the ROI to identical positions in images obtained at different time points or with different flip angles. Slight manual corrections were made to ensure proper alignment with the relevant anatomy in the cases where misregistration occurred from variability in breath-hold position.

For evaluation of flip angle optimization (sequence 2), ROIs were placed in liver tissue (3 ROIs), muscle, right hepatic vein (HV), pre-hepatic portal vein (PV), common hepatic bile duct (CHD), the base of the gall bladder (GB), and in an artifact-free area outside the body (air). Muscle was used as a surrogate tissue for non-hepatocellular liver tumors (26). In order to compensate for possible signal variations due to coil sensitivity variation in larger volunteers, the average SNR of the three liver ROIs was used in all subjects. For dynamic phase and time course image analysis (sequence 1), an additional ROI was placed in the aorta (Ao) to account for arterial contrast enhancement.

Data Analysis – Calculation of SNR, CNR, and Relative CNR

Absolute SNR measurements were made for the time course evaluation data (sequence 1). SNR was calculated as

$$SNR = \frac{S}{\sigma_{mag}} x\, 0.7049 \qquad \text{(Eq. 1)}$$

where S is the average sum-of-squares magnitude signal intensity in tissues of interest and σ_{mag} equals the standard deviation of the background signal measured in areas outside the body not compromised by artifacts. The correction factor of 0.7049 was used to account for differences in the behavior of the noise variance in the background region in magnitude images acquired with multi-channel coils (27–28). CNR calculations were performed in order to compare the contrast of tissues to the liver parenchyma, which is of higher clinical importance than SNR in most typical diagnostic tasks in liver MRI, using the equation

$$CNR = |SNR_{liver} - SNR_{tissue}| \qquad \text{(Eq. 2)}$$

For optimization of flip angle (sequence 2, with parallel imaging), relative contrast-to-noise referenced to non-enhanced liver tissue, rather than absolute SNR and CNR measurements, was calculated because spatially varying noise in parallel imaging compromises absolute SNR and CNR measurements (22–23). For hepatobiliary phase imaging, the flip angle should be optimized to maximize relative contrast between three pairs of tissue: liver and bile ducts, liver and non-enhancing tumors (using muscle as a surrogate), and liver and blood vessels.

Therefore, relative CNR (CNR_{rel}) was calculated as

$$CNR_{rel} = \frac{SI_{liver|post} - SI_{tissue|post}}{SI_{liver|pre}} \quad \text{(Eq. 3)}$$

where $SI_{tissue|post}$ is the signal intensity of the tissue of interest in the hepatobiliary phase, $SI_{liver|post}$ is the signal intensity of liver in the hepatobiliary phase, and $SI_{liver|pre}$ is the signal intensity of liver tissue before contrast injection.

Determination of the optimal flip angle for hepatobiliary phase imaging from the overall group of subjects was performed as follows: for each volunteer, CNR_{rel} was plotted against flip angle for each tissue measured, and the flip angle that maximizes CNR_{rel} was determined. Data from all subjects were then pooled, binning by the optimal flip angle, and finally plotted as a histogram, each bar representing the number of subjects with the particular optimum flip angle. Optimal flip angles for comparable structures (hepatic vein and portal vein; gallbladder and common hepatic duct) were pooled.

Statistical Evaluation

Age and body weight of the subjects are reported as mean ± standard deviation over all subjects. In order to express the variability of the mean of measurements, SNR and CNR measurements are presented as mean ± 95% confidence interval if not stated otherwise. Statistical comparison of CNR_{rel}, SNR, and CNR was performed using paired two-sided Student t-tests using p=0.05 as the threshold for significance.

RESULTS

SNR and CNR Analysis

During the *dynamic phases* (arterial[during maximum arterial enhancement], portal venous [50 sec after maximum enhancement], and venous [2 min after maximum enhancement], gadobenate dimeglumine images showed higher SNR than gadoxetic acid images in liver, muscle and all vascular regions (Table 2), with the exception of the liver during the portal venous phase. However, these differences were not statistically significant except for in the portal and hepatic veins during the portal venous phase (hepatic vein: 104.3 ± 14.7 vs. 76.6 ± 15.2 [p=0.015] in the portal venous phase and 91.3 ± 14.3 vs. 62.4 ± 12.7 [p=0.006] in the venous phase; portal vein: 117.4 ± 10.4 vs. 94.5 ± 15.2 [p=0.013] in the portal venous phase and 106.5 ± 12.5 vs. 78.9 ± 16.3 [p=0.01] in the venous phase). Differences in the aorta in the portal venous phase did not quite reach significance at the $p<0.05$ level (81.1 ± 14.0 vs. 60.1 ± 15.4, p=0.053) (Table 2, Figure 2). Biliary signal and contrast in the dynamic phase are meaningless since there is no contrast in the bile ducts and were therefore excluded from Table 2.

In contrast to SNR, CNR of dynamic phase images performed with gadoxetic acid were slightly higher during venous and portal venous phase than the CNR achieved with gadobenate dimeglumine while they were similar or decreased in the arterial phase. Statistically significant CNR differences, were observed in the portal venous phase for the hepatic vein vs. liver (57.2 ± 66.1 vs. 15.0 ± 16.7 [p=0.026]) and in the venous phase for all three vascular territories: hepatic vein vs. liver (41.4 ± 10.4 vs. 15.1 ± 16.1 [p=0.009]), portal vein vs. liver (24.8 ± 11.7 vs. 0.04 ± 18.8 [p=0.031]), and aorta vs. liver (53.0 ± 17.3 vs. 32.6 ± 19.5 [p=0.050]).

For the *extended time course,* differences in SNR and CNR between the two agents were more pronounced. The time course of SNR and CNR for all evaluated ROIs are provided in Figures 3, 4, and 5. Gadoxetic acid-based liver enhancement was superior to gadobenate dimeglumine during all acquired time points in the extended time course (see Figure 3).

SNR measured in muscle showed similar values for both agents with a tendency toward higher performance with gadobenate dimeglumine although this was not statistically significant. The CNR of muscle (as a surrogate for non-hepatocellular tumor tissue) vs. liver, however, was significantly higher for gadoxetic acid due to the higher liver SNR.

Results for the aorta (Ao), portal vein (PV), and hepatic vein (HV) during the extended time course showed similar results. The lower SNR observed with gadoxetic acid enhanced imaging of these structures, combined with the higher liver SNR, led to statistically significant higher CNR of vessels vs. liver when using gadoxetic acid (Figure 4a–c).

With respect to biliary imaging, contrast arrived earlier in the common hepatic duct and gallbladder when using gadoxetic acid resulting in an early, statistically significant increase of SNR that was superior to gadobenate dimeglumine and persisted throughout the extended time course (Figure 5). Although the SNR performance of gadoxetic acid was superior, the CNR between liver and biliary system was similar for both agents. While CNR values appeared slightly higher in the gallbladder between 25 and 55 minutes when using gadoxetic acid and in the biliary tree after 35 minutes when using gadobenate dimeglumine, these apparent differences were not statistically significant.

Flip Angle Optimization

Figure 6 shows the typical variation in image signal and contrast across a range of flip angles for the two contrast agents in the same volunteer. There were differences in the flip angle behavior for different tissues and different subjects. Figure 7a (upper left) shows a typical optimization plot in a single volunteer, showing how the optimum flip angles were determined for one subject using gadoxetic acid. This procedure was performed for all subjects and the results were binned, as described in the methods section, and displayed in Figure 7b–d. Relative vessel to liver contrast was highest at 25° and 30° for gadoxetic acid and at 15° for gadobenate dimeglumine (Figure 7b). Relative muscle to liver contrast (simulating contrast between non-hepatocellular tumor and liver) was best at 25–30° for gadoxetic acid and 25–30° for gadobenate dimeglumine (Figure 7c). The biliary tree had the best CNR_{rel} relative to liver when using a 45° flip angle with gadoxetic acid and using a 20° flip angle with gadobenate dimeglumine (Figure 7d).

DISCUSSION

There were two goals of this study. First, the SNR and CNR performance of gadoxetic acid and gadobenate dimeglumine was compared at 3T using a cross-over (intra-individual) study design. Overall, from both an SNR and CNR performance perspective, both agents provide adequate enhancement for dynamic phase liver imaging. During the dynamic phase, the SNR and CNR performance of 0.1 mmol/kg of gadobenate dimeglumine was similar to or slightly better than 0.05 mmol/kg of gadoxetic acid in most tested territories and time points, despite the fact that both agents show similar relaxivities and the dose of gadoxetic acid is twice the approved package insert dose. Only the CNR vs. liver tissue vs. PV in the portal venous phase and all three vascular territories in the venous phase showed superiority of gadoxetic acid. These results confirm our anecdotal experience, as well as the experience of other recent investigators (6,12–13) that 0.05 mmol/kg of gadoxetic acid may be necessary to obtain adequate enhancement during the dynamic phase.

During hepatobiliary phase imaging, gadoxetic acid enhanced imaging demonstrated superior SNR performance, although CNR of biliary structures vs. liver was similar between the two agents. Further, the earlier enhancement seen with gadoxetic acid and its higher SNR performance in the biliary phase may make this agent more advantageous for evaluation of bile ducts and characterization of liver lesions during the delayed hepatobiliary

phase. Therefore, we conclude that gadoxetic acid is the preferred agent when delayed hepatobiliary phase imaging is the primary indication for imaging, and that gadobenate dimeglumine is the preferred agent when dynamic phase and vascular imaging is the primary indication for imaging.

Second, this study demonstrates that high-resolution contrast-enhanced hepatobiliary MRI at 3T can benefit tremendously from the use of optimized flip angles, which depends on the contrast agent used and the tissue of interest. Significant relative CNR improvement was achieved by simply increasing the flip angle to the appropriate level. Our findings suggest that during the delayed phase, parameters should be adapted to the structures of interest and the contrast agent used. For example, for biliary imaging, flip angles of 45° and 20° were optimal for gadoxetic acid and gadobenate dimeglumine, respectively. Previous studies that studied these agents during the hepatobiliary phase used a variety of gradient echo pulse sequences using either GRE with high flip angles (8–9,11,29–31), low flip angles of 10–15° at 1.5T (2,32–35), or did not report flip angles at all (7,12,26). Similarly, protocols designed for higher spatial resolution, e.g., using navigator-gated approaches to compensate for breathing motion, did not employ optimized flip angles (36).

A dose of 0.05 mmol/kg gadoxetic acid (twice the approved package insert dose) was used for comparison with 0.1 mmol/kg of gadobenate dimeglumine in this study. It is important to note that gadoxetic acid was approved for use at the minimum effective dose for detection and characterization of liver lesions in the delayed hepatobiliary phase (0.025 mmol/kg) with lesser regard to its performance for dynamic phase imaging. Based on our anecdotal experience and a growing body of literature (6,12–13), a dose of 0.025 mmol/kg may provide inferior enhancement during the dynamic phase, compared to other agents. The results of this study support our clinical observations as well as the literature, i.e., that 0.05 mmol/kg of gadoxetic acid may be a more appropriate dose for dynamic phase imaging, comparable to other agents. Further, it should be noted that the use of gadobenate dimeglumine (at any dose) is off-label for hepatobiliary imaging in the United States, although liver imaging at 0.1 mmol/kg of gadobenate dimeglumine is approved in Europe.

A weakness of this study is that only healthy subjects were included in the analysis. We expect that different liver diseases may result in different optimal scan parameters, especially in the setting of liver failure when there is compromised hepatic uptake and biliary excretion. However, the use of standard protocols, optimized to normal hepatic uptake and biliary excretion can be very helpful in identifying abnormalities in uptake and excretion in the presence of disease (e.g., in primary sclerosing cholangitis (37)). Also, the presence of cholestasis and drugs that interfere with biliary uptake and excretion could potentially alter the enhancement patterns seen with both gadobenate dimeglumine and gadoxetic acid (38). Although such changes may contain important diagnostic information, future work will ne needed to extend this analysis into the setting of liver disease.

Further, a direct SNR and CNR comparison, optimally would have been compared *after* the optimization of flip angles. This would require a second study with an additional group of subjects and contrast, which was impractical due to limited resources. However, it is well known that the signal intensity of spoiled gradient echo imaging methods increases monotonically as gadolinium concentration increases in tissue. Using optimized and/or fixed flip angles to compare the two agents would not change the relative performance of one agent over another, but simply change the size of that difference. Furthermore, it is not possible or practical to ascertain the optimum flip angle at all different phases of contrast. Therefore, the use of a fixed 15° flip angle to compare the SNR and CNR performance of gadoxetic acid and gadobenate dimeglumine is valid, and can be used to determine equivalency or superiority of an agent. Finally, our study did not investigate the use of flip

angles greater than 45°, which was the maximum possible flip angle due to technical constraints. It therefore remains unclear, whether image quality would benefit from a further increase of the flip angle, especially when using gadoxetic acid.

In conclusion, this is, to the best of our knowledge, the first study comparing the performance of 0.05 mmol/kg of gadoxetic acid and 0.1 mmol/kg of gadobenate dimeglumine in the liver at 3T. The SNR and CNR performance of gadobenate dimeglumine and gadoxetic acid during the dynamic phase demonstrated a small SNR-advantage using gadobenate dimeglumine despite the use of 0.05 mmol/kg of gadoxetic acid. During the extended time course, gadoxetic acid demonstrated equal or superior SNR-performance in the liver and biliary tract while the SNR of gadobenate dimeglumine was equal or superior in vessels. Based on these findings we conclude that while 0.1 mmol/kg of gadobenate dimeglumine is superior for dynamic phase imaging, 0.05 mmol/kg of gadoxetic acid is probably adequate. The results further confirm that in extended time course imaging, gadoxetic acid provides earlier and superior hepatic and biliary enhancement relative to gadobenate dimeglumine. Finally, the use of optimized flip angles can provide markedly improved relative CNR performance in the delayed hepatobiliary phase at 3T.

Acknowledgments

Grant support: The authors gratefully acknowledge support from NIH (R01 DK083380, R01 DK088925 and RC1 EB010384), the Coulter Foundation, Bracco Diagnostics, and GE Healthcare.

The authors would like to thank Kelli Hellenbrand and Sara Pladziewicz for their assistance. The authors gratefully acknowledge support from Bracco Diagnostics, GE Healthcare, NIH, and the Coulter Foundation.

References

1. Huppertz A, Haraida S, Kraus A, et al. Enhancement of focal liver lesions at gadoxetic acid-enhanced MR imaging: correlation with histopathologic findings and spiral CT--initial observations. Radiology. 2005; 234(2):468–478. [PubMed: 15591431]
2. Grazioli L, Morana G, Kirchin MA, Schneider G. Accurate differentiation of focal nodular hyperplasia from hepatic adenoma at gadobenate dimeglumine-enhanced MR imaging: prospective study. Radiology. 2005; 236(1):166–177. [PubMed: 15955857]
3. Bluemke DA, Sahani D, Amendola M, et al. Efficacy and safety of MR imaging with liver-specific contrast agent: U.S. multicenter phase III study. Radiology. 2005; 237(1):89–98. [PubMed: 16126918]
4. Hammerstingl R, Huppertz A, Breuer J, et al. Diagnostic efficacy of gadoxetic acid (Primovist)-enhanced MRI and spiral CT for a therapeutic strategy: comparison with intraoperative and histopathologic findings in focal liver lesions. Eur Radiol. 2008; 18(3):457–467. [PubMed: 18058107]
5. Raman SS, Leary C, Bluemke DA, et al. Improved characterization of focal liver lesions with liver-specific gadoxetic acid disodium-enhanced magnetic resonance imaging: a multicenter phase 3 clinical trial. J Comput Assist Tomogr. 2010; 34(2):163–172. [PubMed: 20351497]
6. Lee MS, Lee JY, Kim SH, et al. Gadoxetic acid disodium-enhanced magnetic resonance imaging for biliary and vascular evaluations in preoperative living liver donors: Comparison with gadobenate dimeglumine-enhanced MRI. J Magn Reson Imaging. 2011; 33(1):149–159. [PubMed: 21182133]
7. Dahlstrom N, Persson A, Albiin N, Smedby O, Brismar TB. Contrast-enhanced magnetic resonance cholangiography with Gd-BOPTA and Gd-EOB-DTPA in healthy subjects. Acta Radiol. 2007; 48(4):362–368. [PubMed: 17453513]
8. Reimer P, Rummeny EJ, Shamsi K, et al. Phase II clinical evaluation of Gd-EOB-DTPA: dose, safety aspects, and pulse sequence. Radiology. 1996; 199(1):177–183. [PubMed: 8633143]
9. Vogl TJ, Pegios W, McMahon C, et al. Gadobenate dimeglumine--a new contrast agent for MR imaging: preliminary evaluation in healthy volunteers. AJR Am J Roentgenol. 1992; 158(4):887–892. [PubMed: 1546612]

10. Schuhmann-Giampieri G. Liver contrast media for magnetic resonance imaging. Interrelations between pharmacokinetics and imaging. Invest Radiol. 1993; 28(8):753– 761. [PubMed: 8376008]
11. Hamm B, Staks T, Muhler A, et al. Phase I clinical evaluation of Gd-EOB-DTPA as a hepatobiliary MR contrast agent: safety, pharmacokinetics, and MR imaging. Radiology. 1995; 195(3):785–792. [PubMed: 7754011]
12. Brismar TB, Dahlstrom N, Edsborg N, Persson A, Smedby O, Albiin N. Liver vessel enhancement by Gd-BOPTA and Gd-EOB-DTPA: a comparison in healthy volunteers. Acta Radiol. 2009; 50(7):709–715. [PubMed: 19701821]
13. Motosugi U, Ichikawa T, Sano K, et al. Double-Dose Gadoxetic Acid-Enhanced Magnetic Resonance Imaging in Patients With Chronic Liver Disease. Invest Radiol. 2010
14. Rohrer M, Bauer H, Mintorovitch J, Requardt M, Weinmann HJ. Comparison of magnetic properties of MRI contrast media solutions at different magnetic field strengths. Invest Radiol. 2005; 40(11):715–724. [PubMed: 16230904]
15. Winterer JT, Moske-Eick O, Markl M, Frydrychowicz A, Bley TA, Langer M. Bilateral ce-MR angiography of the hands at 3.0 T and 1. 5 T: intraindividual comparison of quantitative and qualitative image parameters in healthy volunteers. Eur Radiol. 2008; 18(4):658–664. [PubMed: 18040693]
16. Stalder AF, Elverfeldt DV, Paul D, Hennig J, Markl M. Variable echo time imaging: signal characteristics of 1-M gadobutrol contrast agent at 1. 5 and 3T. Magn Reson Med. 2008; 59(1): 113–123. [PubMed: 18058940]
17. Cashen TA, Carr JC, Shin W, et al. Intracranial time-resolved contrast-enhanced MR angiography at 3T. AJNR Am J Neuroradiol. 2006; 27(4):822–829. [PubMed: 16611772]
18. Merkle EM, Dale BM, Barboriak DP. Gain in signal-to-noise for first-pass contrast-enhanced abdominal MR angiography at 3 Tesla over standard 1. 5 Tesla: prediction with a computer model. Acad Radiol. 2007; 14(7):795–803. [PubMed: 17574130]
19. Michaely HJ, Kramer H, Dietrich O, et al. Intraindividual comparison of high-spatial-resolution abdominal MR angiography at 1.5 T and 3. 0 T: initial experience. Radiology. 2007; 244(3):907–913. [PubMed: 17709837]
20. Nagle SN, Busse RF, Brau AC, et al. High-Resolution Free-Breathing 3D T1 Weighted Hepatobiliary Imaging Optimized for Gd-EOB-DTPA. Proceedings of the Intl Soc Magn Reson Med. 2009; 17:2076.
21. Bashir MR, Merkle EM. Improved liver lesion conspicuity by increasing the flip angle during hepatocyte phase MR imaging. Eur Radiol. 2010
22. Pruessmann KP, Weiger M, Scheidegger MB, Boesiger P. SENSE: sensitivity encoding for fast MRI. Magn Reson Med. 1999; 42(5):952–962. [PubMed: 10542355]
23. Reeder SB, Wintersperger BJ, Dietrich O, et al. Practical approaches to the evaluation of signal-to-noise ratio performance with parallel imaging: application with cardiac imaging and a 32-channel cardiac coil. Magn Reson Med. 2005; 54(3):748–754. [PubMed: 16088885]
24. Prince MR, Chenevert TL, Foo TK, Londy FJ, Ward JS, Maki JH. Contrast-enhanced abdominal MR angiography: optimization of imaging delay time by automating the detection of contrast material arrival in the aorta. Radiology. 1997; 203(1):109–114. [PubMed: 9122376]
25. Brau AC, Beatty PJ, Skare S, Bammer R. Comparison of reconstruction accuracy and efficiency among autocalibrating data-driven parallel imaging methods. Magn Reson Med. 2008; 59(2):382–395. [PubMed: 18228603]
26. Runge VM. A comparison of two MR hepatobiliary gadolinium chelates: Gd-BOPTA and Gd-EOB-DTPA. J Comput Assist Tomogr. 1998; 22(4):643–650. [PubMed: 9676461]
27. Constantinides CD, Atalar E, McVeigh ER. Signal-to-noise measurements in magnitude images from NMR phased arrays. Magn Reson Med. 1997; 38(5):852–857. [PubMed: 9358462]
28. Dietrich O, Raya JG, Reeder SB, Ingrisch M, Reiser MF, Schoenberg SO. Influence of multichannel combination, parallel imaging and other reconstruction techniques on MRI noise characteristics. Magn Reson Imaging. 2008; 26(6):754–762. [PubMed: 18440746]
29. Manfredi R, Maresca G, Baron RL, et al. Delayed MR imaging of hepatocellular carcinoma enhanced by gadobenate dimeglumine (Gd-BOPTA). J Magn Reson Imaging. 1999; 9(5):704–710. [PubMed: 10331767]

30. Petersein J, Spinazzi A, Giovagnoni A, et al. Focal liver lesions: evaluation of the efficacy of gadobenate dimeglumine in MR imaging--a multicenter phase III clinical study. Radiology. 2000; 215(3):727–736. [PubMed: 10831691]

31. Schima W, Petersein J, Hahn PF, Harisinghani M, Halpern E, Saini S. Contrast-enhanced MR imaging of the liver: comparison between Gd-BOPTA and Mangafodipir. J Magn Reson Imaging. 1997; 7(1):130–135. [PubMed: 9039603]

32. Tschirch FT, Struwe A, Petrowsky H, Kakales I, Marincek B, Weishaupt D. Contrast-enhanced MR cholangiography with Gd-EOB-DTPA in patients with liver cirrhosis: visualization of the biliary ducts in comparison with patients with normal liver parenchyma. Eur Radiol. 2008; 18(8): 1577–1586. [PubMed: 18369632]

33. Kim JI, Lee JM, Choi JY, et al. The value of gadobenate dimeglumine-enhanced delayed phase MR imaging for characterization of hepatocellular nodules in the cirrhotic liver. Invest Radiol. 2008; 43(3):202–210. [PubMed: 18301317]

34. Kim YK, Lee JM, Kim CS. Gadobenate dimeglumine-enhanced liver MR imaging: value of dynamic and delayed imaging for the characterization and detection of focal liver lesions. Eur Radiol. 2004; 14(1):5–13. [PubMed: 14600778]

35. Marin D, Di Martino M, Guerrisi A, et al. Hepatocellular carcinoma in patients with cirrhosis: qualitative comparison of gadobenate dimeglumine-enhanced MR imaging and multiphasic 64-section CT. Radiology. 2009; 251(1):85–95. [PubMed: 19332848]

36. Asbach P, Warmuth C, Stemmer A, et al. High spatial resolution T1-weighted MR imaging of liver and biliary tract during uptake phase of a hepatocyte-specific contrast medium. Invest Radiol. 2008; 43(11):809–815. [PubMed: 18923261]

37. Jedynak AR, Kelcz F, Frydrychowicz A, Nagle SN, Reeder SB. Clinical Experience with Gadoxetate-Enhanced T1 Weighted Hepatobiliary Imaging in Primary Sclerosing Cholangitis. Proc Intl Soc Magn Reson Med. 2010; 18:2620.

38. van Montfoort JE, Stieger B, Meijer DK, Weinmann HJ, Meier PJ, Fattinger KE. Hepatic uptake of the magnetic resonance imaging contrast agent gadoxetate by the organic anion transporting polypeptide Oatp1. J Pharmacol Exp Ther. 1999; 290(1):153–157. [PubMed: 10381771]

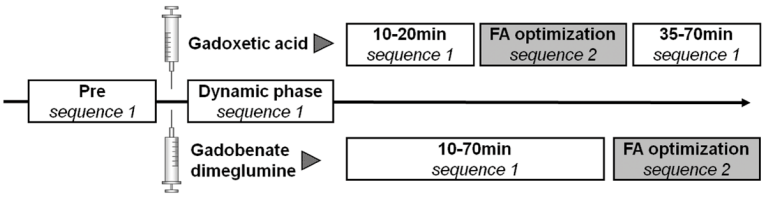

Figure 1.

Overview of the study design. After study setup, preparation, and pre-contrast imaging (Pre), dynamic and time course acquisitions were performed using sequence 1 without parallel imaging, interrupted by a series of flip angle optimization scans using parallel imaging (sequence 2) at 20–30 minutes for gadoxetic acid and 75–90 min for gadobenate dimeglumine.

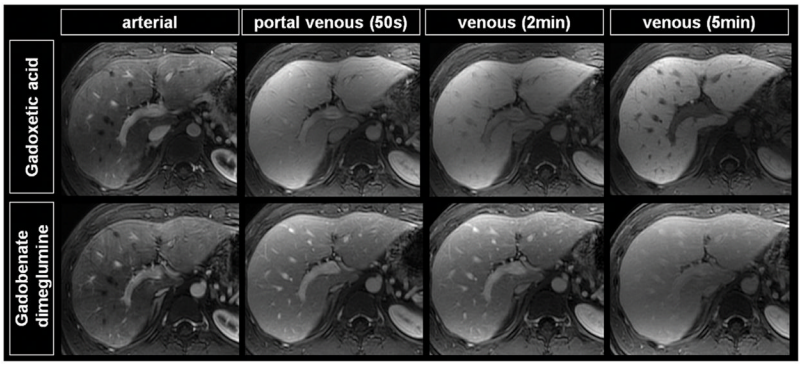

Figure 2.

Comparison of dynamic phase images from a typical subject imaged with gadoxetic acid (top row) and gadobenate dimeglumine (bottom row). The SNR and CNR performance of gadobenate dimeglumine and gadoxetic acid during the dynamic phase are similar. However, slightly pronounced liver SNR translates into superior vessel and muscle CNR relative to liver.

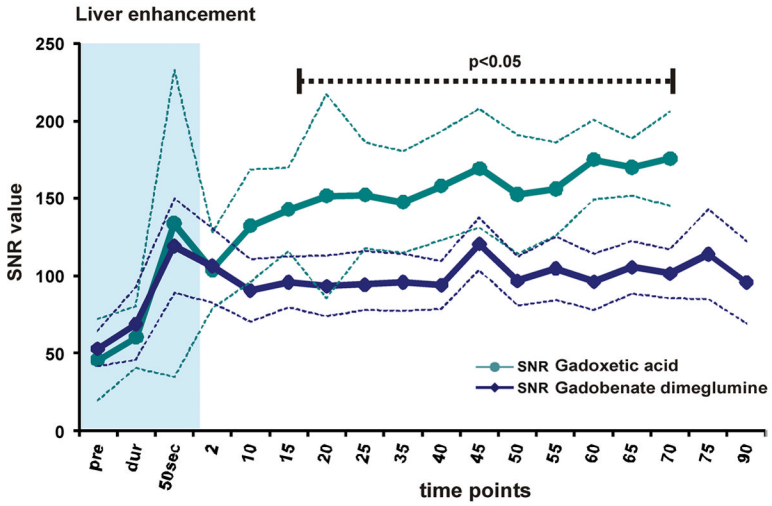

Figure 3.

(A) SNR of liver and (B) SNR and CNR muscle vs liver tissue. SNR is displayed by solid lines, CNR by dashed lines with data points. Thin dashed lines represent average ± 95% confidence interval over all subjects. Liver SNR with both agents is similar during the dynamic phase, and shows advantages for gadoxetic acid during the delayed phase. Muscle enhancement shows overall similar values. However, CNR of muscle vs. liver of gadoxetic acid is superior throughout most of the time course. Significance levels are indicated where differences showed statistical significance to the $p<0.05$ level. The blue shaded area represents the dynamic phase. Due to study design, measurements at 5 and 30 minutes were not acquired.

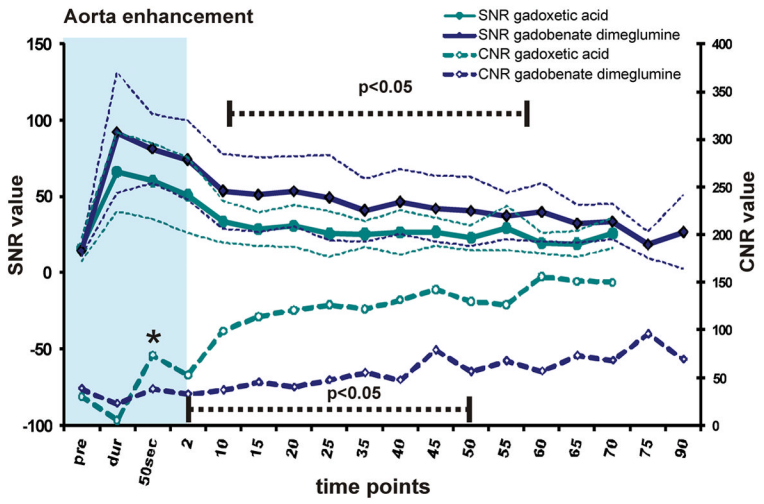

Figure 4.

SNR and CNR versus liver tissue for (A) the aorta, (B) the portal vein, and (C) the hepatic vein. SNR is displayed by solid lines, CNR by dashed lines with data points. Thin dashed lines represent average ± 95% confidence interval over all subjects. Gadobenate dimeglumine images demonstrated slightly higher SNR. CNR of vessels vs. liver, however, was greater using gadoxetic acid in the delayed phase. Significance levels are indicated (dashed black line, asterisk) where differences showed statistically significance to the $p<0.05$ level. The blue shaded area represents the dynamic phase. Due to study design, measurements at 5 and 30 minutes were not acquired.

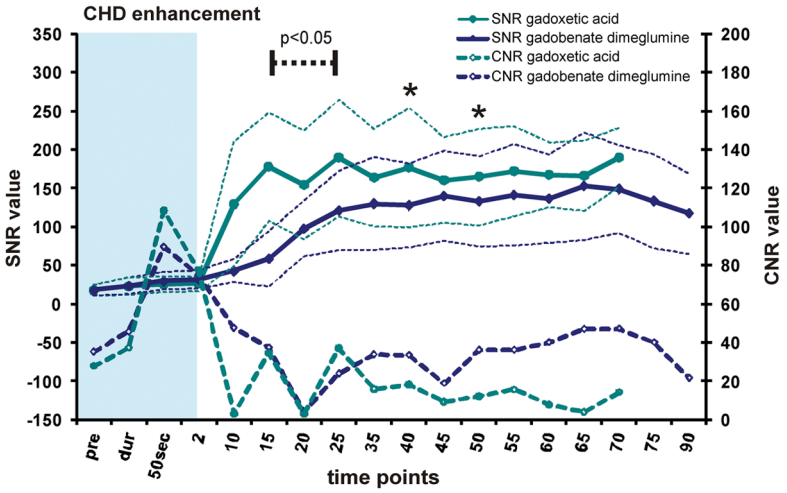

Figure 5.

SNR and CNR versus liver tissue for (A) the common hepatic duct and (B) the gall bladder. SNR is displayed by solid lines, CNR by dashed lines with data points. Thin dashed lines represent average ± 95% confidence interval over all subjects. Images acquired using gadoxetic acid show superior SNR in the extended time course. CNR of vessels vs. liver with gadoxetic acid and gadobenate was similar during the delayed phase. Significance levels are indicated (dashed black line, asterisk) where differences showed statistically significance to the $p<0.05$ level. The blue shaded area represents the dynamic phase. Due to study design, measurements at 5 and 30 minutes were not acquired.

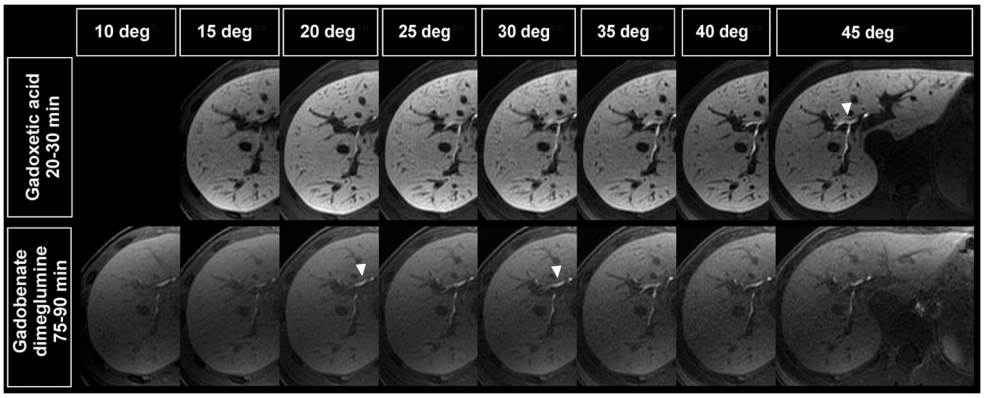

Figure 6.
Comparison of image quality in delayed images from the same subject at different flip angles for gadoxetic acid (upper row) acquired at 20–30 min and gadobenate dimeglumine (lower row) acquired at 75–90 min. Gadoxetic acid enhanced imaging demonstrates improved enhancement with higher SNR in the liver, compared to gadobenate dimeglumine, in the delayed hepatobiliary phase. White arrowheads indicate which flip angle showed best relative signal differences to liver parenchyma regarding hepatobiliary enhancement.

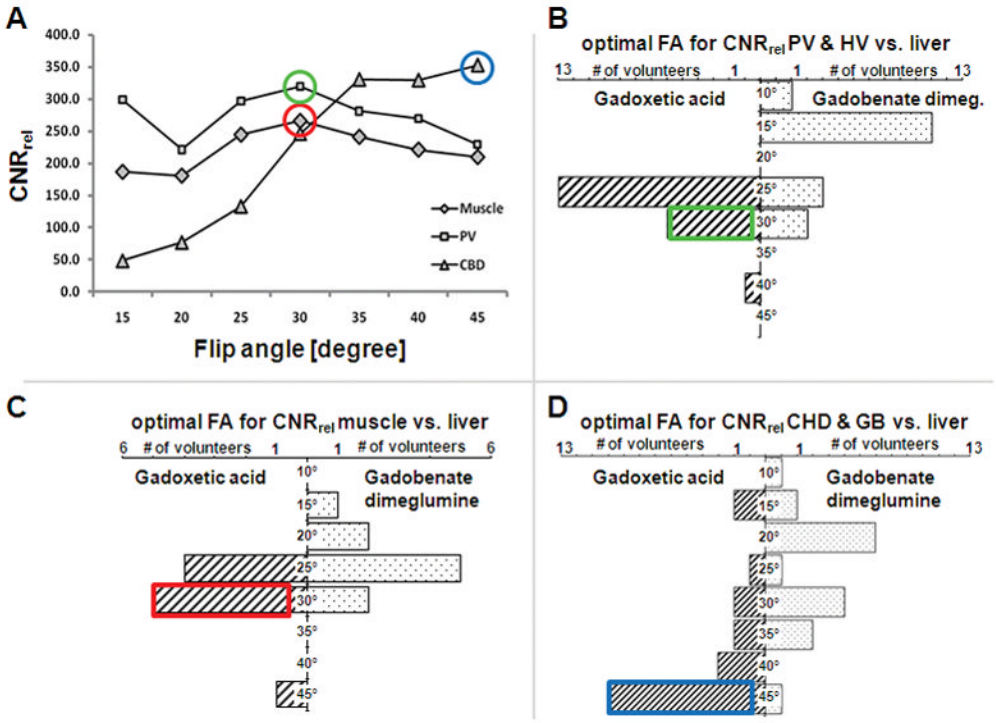

Figure 7.

Distribution of optimal flip angles by means of CNR_{rel} compared to liver tissue. (A) plots of flip angle vs. CNR_{rel} using gadoxetic acid in a single volunteer. The optimal flip angle was determined in every volunteer for both agents. Data from all volunteers was then binned into the plots for imaging vessels (B; PV=portal vein, HV = hepatic vein), muscle (as a surrogate for non-hepatocellular tumor tissue, C), and biliary tree (D; GB = gallbladder, CHD = common hepatic duct).

Table 1

Sequence parameters for imaging during the dynamic phase and extended time course (sequence 1) and flip angle optimization (sequence 2)

	Sequence 1	Sequence 2
Parallel Imaging?	no	yes
Type of parallel imaging [acceleration factor]	n/a	ARC (25) [R=3.56]
main purpose	dynamic phase & time course imaging	flip angle optimization high resolution imaging
parameters to evaluate	SNR, CNR	CNR_{rel} relative contrast-to-noise
sequence type	3D SPGR (LAVA)	3D SPGR (LAVA)
fat saturation	periodic spectrally-selective partial inversion	periodic spectrally-selective partial inversion
excitation	axial slab excitation	axial slab excitation
FA	15°	5° steps from 10°–45°
TR	4.1 ms	5.4–5.5 ms
TE	1.8 ms	2.1 ms
matrix	256 × 192	288 × 224
FOV	400 × 320	400 × 320
BW	±62.5 kHz	±62.5 kHz
slices	80	192
slice thickness	5 mm	2 mm
true spatial resolution	1.6 × 2.1 × 5 mm^3	1.4 × 1.8 × 2.0 mm^3
interpolated spatial resolution	0.8 × 0.8 × 2.5 mm^3	0.8 × 0.8 × 1.0 mm^3

Tab. 2

SNR and CNR measurements from the dynamic phases with Gadoxetic acid and Gadobenate dimeglumine (values are given as mean ± 95% CI over all subjects). CNR was calculated relative to liver tissue. Results shown include only muscle, vascular, and liver evaluations because gallbladder and common hepatic duct do not enhance during these dynamic phases

		Imaging Phase							
		pre		arterial		portal venous		venous	
SNR		**mean ± CI**	**p**	**mean ± CI**	**p**	**mean ± CI**	**p**	**mean ± CI**	**p**
Liver	gadoxetic acid	45.8 ± 7.6		60.4 ± 12.2		133.7 ± 61.4		103.7 ± 15.1	
	gadobenate dimeglumine	53.2 ± 7.0	0.104	69 ± 14.4	0.305	119.3 ± 18.8	0.654	106.5 ± 14.9	0.800
Ao	gadoxetic acid	15.7 ± 4.9		66 ± 15.9		60.1 ± 15.4		50.8 ± 15.5	
	gadobenate dimeglumine	14.6 ± 2.1	0.682	91.8 ± 24.5	0.180	81.1 ± 14.0	0.053	73.9 ± 15.9	0.072
PV	gadoxetic acid	20.1 ± 3.4		106.9 ± 20.5		94.5 ± 15.2		78.9 ± 16.3	
	gadobenate dimeglumine	21.8 ± 2.4	0.190	109.1 ± 28.8	0.911	**117.4 ± 10.4**	**0.013**	**106.5 ± 12.5**	**0.010**
HV	gadoxetic acid	16.4 ± 3.0		29.3 ± 11.3		76.6 ± 13.9		62.4 ± 12.7	
	gadobenate dimeglumine	17.6 ± 2.5	0.445	34.8 ± 13.4	0.620	**104.3 ± 14.7**	**0.015**	**91.3 ± 14.3**	**0.006**
Muscle	gadoxetic acid	44.4 ± 11.0		50.3 ± 14.0		58.5 ± 19.4		57.6 ± 19.7	
	gadobenate dimeglumine	56.9 ± 8.6	0.139	59 ± 11.1	0.445	73.0 ± 12.9	0.319	74.9 ± 12.8	0.261
CNR									
Ao	gadoxetic acid	30.1 ± 8.5		5.5 ± 14.0		73.6 ± 63.9		**53.0± 17.3**	
	gadobenate dimeglumine	38.6 ± 6.7	0.202	22.8 ± 26.8	0.313	38.2 ± 21.5	0.148	32.6 ± 19.5	**0.050**
PV	gadoxetic acid	25.7 ± 5.8		46.5 ± 9.8		39.2 ± 60.4		**24.8 ± 11.7**	
	gadobenate dimeglumine	31.4 ± 6.5	0.376	40 ± 26.4	0.491	1.9 ± 19.2	0.112	0.04 ± 18.9	**0.031**
HV	gadoxetic acid	29.4 ± 6.5		31.1 ± 13.0		**57.2 ± 66.1**		**41.4 ± 10.4**	
	gadobenate dimeglumine	35.5 ± 7.2	0.405	34.2 ± 21.7	0.687	15.0 ± 16.7	**0.026**	15.1 ± 16.1	**0.009**

		Imaging Phase							
		pre		arterial		portal venous		venous	
SNR		**mean ± CI**	**p**	**mean ± CI**	**p**	**mean ± CI**	**p**	**mean ± CI**	**p**
Muscle	gadoxetic acid	1.4 ± 11.1		10.2 ± 16.4		75.2 ± 66.4		46.1 ± 16.7	
	gadobenate dimeglumine	3.8 ± 14.2	0.449	10.1 ± 17.7	0.718	46.3 ± 24.6	0.377	31.6 ± 21.5	0.181

Ao = aorta, PV = portal vein, HV = hepatic vein. Bold type indicates statistical significance in comparison to the other contrast agent with p<0.05.